Characterization of Tescalcin, a Novel EF-Hand Protein with a Single Ca^{2+}-Binding Site: Metal-Binding Properties, Localization in Tissues and Cells, and Effect on Calcineurin†

Christina Gutierrez-Ford,‡ Konstantin Levay,‡ Aldrin V. Gomes,‡ Erasmo M. Perera,§ Tapan Som,|| You-Me Kim,|| Jeffrey L. Benovic,|| Gary D. Berkovitz,§ and Vladlen Z. Slepak*,‡

Department of Molecular and Cellular Pharmacology and Pediatric Endocrinology, University of Miami School of Medicine, Miami, Florida 33136, and The Kimmel Cancer Center, Department of Microbiology and Immunology, Thomas Jefferson University, Philadelphia, Pennsylvania 19107

Received May 23, 2003; Revised Manuscript Received September 3, 2003

ABSTRACT: The tescalcin gene is preferentially expressed during mouse testis differentiation. Here, we demonstrate that this gene encodes a 24 kDa Ca^{2+}- and Mg^{2+}-binding protein with one consensus EF-hand and three additional domains with EF-hand homology. Equilibrium dialysis with $^{45}Ca^{2+}$ revealed that recombinant tescalcin binds approximately one Ca^{2+} ion at physiological concentrations (pCa 4.5). The intrinsic tryptophan fluorescence of tescalcin was significantly reduced by Ca^{2+}, indicative of a conformational change. The apparent K_d for Ca^{2+} was 0.8 μM. A point mutation in the consensus EF-hand (D123A) abolished $^{45}Ca^{2+}$ binding and prevented the fluorescence quenching, demonstrating that the consensus EF-hand alone mediates the Ca^{2+}-induced conformational change. Tescalcin also binds Mg^{2+} (K_d 73 μM), resulting in a much smaller fluorescence decrease. In the presence of 1 mM Mg^{2+}, tescalcin's Ca^{2+} affinity is shifted to 3.5 μM. These results illustrate that tescalcin should bind Mg^{2+} constitutively in a quiescent cell, replacing it with Ca^{2+} during stimulation. We also show that tescalcin is most abundant in adult mouse heart, brain, and stomach, as well as in HeLa and HL-60 cells. Immunofluorescence microscopy revealed that tescalcin is present in the cytoplasm and nucleus, with concentration in membrane ruffles and lamellipodia in the presence of serum, where it colocalizes with the small guanosine triphosphatase Rac-1. Tescalcin shares sequence and functional homology with calcineurin-B homologous protein (CHP), and we found that tescalcin, like CHP, can inhibit the phosphatase activity of calcineurin A. Hence, tescalcin is a novel calcineurin B-like protein that binds a single Ca^{2+} ion.

Tescalcin (Tsc)[1] was discovered as an autosomal gene preferentially expressed during the early stages of mouse testis development (*1*). Its expression begins at 11.5 days postcoitum (dpc), peaks at 14.5 dpc, and declines at 17.5 dpc, a time when many of the sex-determining genes such as Amh, Sf-1, Wt-1, and Sox9 are expressed and migration of endothelial cells occurs (*1*−*4*). The deduced amino acid sequence of tescalcin bears a consensus EF-hand domain near the C-terminus (region 114−142), an N-myristoylation motif, and several phosphorylation sites.

The consensus EF-hand domain is defined as a 29 amino acid long helix−loop−helix array in which one Ca^{2+} ion is coordinated by six amino acid residues within the loop (*5*). Since Ca^{2+} is a universal intracellular second messenger, Ca^{2+}-binding proteins belonging to the EF-hand superfamily can play critical roles in a diversity of cellular events ranging from nuclear transcription to cellular trafficking to proteolysis (*6*). The Ca^{2+} concentrations within a eukaryotic cell are generally maintained quite low at approximately 10−100 nM, so that they may be rapidly and dynamically increased to 1−10 μM upon receiving a stimulus (*5*). EF-hand Ca^{2+}-binding proteins are classified into two separate groups based on their Ca^{2+} affinity and ability to respond to these rising Ca^{2+} signals. The "Ca^{2+} sensors" such as calmodulin (CaM) possess affinities within the range of stimulatory Ca^{2+}

† This work was supported in part by National Institutes of Health RO1 Grants GM60019 and EY 12982 (to V.Z.S.), as well as GM44944 (to J.L.B.), a Howard Hughes Medical Institute Predoctoral Fellowship (to C.G.-F.), a Stanley Glaser Research Award (to K.L.), and a Florida Department of Health Award (to G.D.B.).

* To whom correspondence should be addressed: University of Miami School of Medicine, R-189, 1600 NW 10th Ave, Miami, FL 33136. Phone (305) 243-3430; fax (305) 243-4555; e-mail v.slepak@miami.edu.

‡ Department of Molecular and Cellular Pharmacology, University of Miami School of Medicine.

§ Department of Pediatric Endocrinology, University of Miami School of Medicine.

|| The Kimmel Cancer Center, Department of Microbiology and Immunology, Thomas Jefferson University.

[1] Abbreviations: Tsc, tescalcin; CHP, calcineurin homologous protein; NHE, sodium−hydrogen exchanger; dpc, days postcoitum. CaM, calmodulin; CnA, calcineurin A; CnB, calcineurin B; CHO, Chinese hamster ovary; PAGE, polyacrylamide gel electrophoresis; PCR, polymerase chain reaction; PBS, phosphate-buffered saline; DMEM, Dulbecco's modified Eagle's medium; NMT, *N*-myristoyl transferase; SD, standard deviation; STI, soybean trypsin inhibitor; MTE, multiple tissue expression; MOPS, 3-(*N*-morpholino)propanesulfonic acid; EDTA, ethylenediaminetetraacetic acid; EGTA, ethylene glycol bis(β-aminoethyl ether)-*N*,*N*,*N*′,*N*′-tetraacetic acid; IPTG, isopropyl β-D-thiogalactoside; NTA, nitrilotriacetate.

10.1021/bi034870f CCC: $25.00
Published on Web 11/14/2003

concentrations of $10^{-5}-10^{-6}$ M and exhibit Ca^{2+}-induced conformational changes, whereas "Ca^{2+} buffers" such as parvalbumin constitutively bind Ca^{2+} with affinities of <100 nM and generally lack a conformational change (*7*). EF-hand domains may also coordinate other divalent cations including Mg^{2+} and Zn^{2+} ions. Most Ca^{2+}-binding proteins contain one or more pairs of EF-hand domains, which imparts stability and often cooperativity. Although at first glance the tescalcin sequence appears to contain solely a single consensus EF-hand domain, closer analysis reveals three other helix−loop−helix regions with moderate EF-hand homology that may endow stability by allowing EF-hand pairing.

Tescalcin shares significant homology with three Ca^{2+}-binding proteins: calcineurin homologous protein 1, CHP1 (also known as p22); CHP2; and calcineurin B, CnB (*8*−*10*). All three aforementioned proteins possess known or putative N-myristoylation motifs. In the EF-hand protein recoverin, this acyl group is extruded in response to Ca^{2+} binding in a major conformational change termed a Ca^{2+}-myristoyl switch that facilitates membrane binding and G protein-coupled receptor kinase 1 (GRK1) inhibition (*11*, *12*).

Calcineurin B forms a heterodimer with the catalytic subunit calcineurin A, a serine/threonine phosphatase. Ca^{2+} binding by CnB is important for the structure rather than regulation of CnA activity. Instead, the phosphatase activity of the heterodimer is activated by the binding of Ca^{2+}-bound calmodulin to CnA (*9*). The prototypical calcineurin substrate is NF-AT, which translocates to the nucleus upon dephosphorylation and thereby exerts transcriptional regulation. CHP1 was shown to inhibit CaM−calcineurin activity and to prevent the associated translocation of NF-AT (*13*). CHP1 also has a role in other cellular processes including vesicular trafficking, association with microtubules, and binding to the apoptosis-linked serine/threonine kinase DRAK2 (*8*, *14*, *15*). CHP1 and -2 were also reported to show Ca^{2+}/myristoylation-independent binding to the sodium−hydrogen exchanger (NHE), which extrudes H^+ ions outside the cell in return for Na^+ ions to maintain proper intracellular pH and volume (*10*, *16*−*18*). CHP1 serves as an essential cofactor to preserve resting NHE1−3 exchange activity in cells (*10*, *17*). A recent study identified binding of NHE to human tescalcin by a yeast two-hybrid screen of a cDNA library with the C-terminal region of NHE1 (*19*); overexpression of tescalcin appears to inhibit the activity of NHE1 (*20*).

Previously, we demonstrated the preferential expression of tescalcin mRNA during testis differentiation as well as its temporal and spatial expression in the testis (*1*). In the present study, we show that the tescalcin gene encodes a 24 kDa cytosolic protein with a restricted tissue pattern that corroborates mRNA expression. Furthermore, we reveal that tescalcin binds a sole Ca^{2+} ion and experiences Ca^{2+}- and Mg^{2+}-induced conformational changes. Finally, we suggest that tescalcin shares homology with the calcineurin B subfamily not only on the basis of sequence homology but also by its inhibition of calcineurin phosphatase activity.

EXPERIMENTAL PROCEDURES

Materials. Restriction enzymes, DNA-modifying enzymes, and Deep Vent polymerase were purchased from New England Biolabs. Deoxynucleoside triphosphates (dNTPs) for PCR amplification were purchased from Roche, Inc. EDTA-free protease inhibitor cocktail (Roche) was supplemented in all cellular and tissue lysates. Protein concentrations were measured by Bio-Rad Bradford protein assay unless otherwise noted. Protein electrophoresis reagents and markers were from Bio-Rad, and DNA markers were from Invitrogen. Cell culture plastic and media were purchased from Costar. Other chemicals were from Sigma. Murine monoclonal anti-HA antibody was from Covance, Inc., and mouse monoclonal actin antibody from Chemicon. Anti-nucleolin (C23) antibody was purchased from Santa Cruz. Secondary anti-mouse and anti-rabbit antibodies were obtained from Jackson Immunologicals.

Gel Electrophoresis and Immunoblotting. Proteins were separated on SDS−12% PAGE and transferred onto nitrocellulose (Schleicher & Schull). Native PAGE was performed in the absence of SDS. Membranes were blocked with 5% fat-free milk in TBST (20 mM Tris, 50 mM NaCl, and 0.3% Tween-20, pH 7.4), incubated with primary antibodies for 1 h at room temperature or overnight at 4 °C (1:1000), and then incubated with horseradish peroxidase- (HRP-) linked secondary antibody for 1 h at room temperature (1:5000). Visualization of protein bands was performed by enhanced chemiluminescence (ECL; Western blotting detection reagent, Amersham Biosciences) and exposure to Kodak X-Omat film.

Construction of Plasmids. The coding sequence for mouse Tsc was PCR-amplified by use of a pair of synthetic oligonucleotides, forward 5′-CTGCA**GTCGAC**ATGGGC-GCTGCCCAC TCG-3′ with a *Sal*I site and reverse 5′-TCTAGA**TGATCA**AGTCAGTGGCAGAGGGCGAT-3′ with a *Bcl*I site, and cloned into a *Xho*I/*Bam*HI-linearized bacterial expression vector pET15b (Novagen) designed to express the fusion protein with a hexahistidine tag at the N-terminus (pTsc-HisN). The coding sequence of wild-type Tsc was PCR-amplified and inserted under control of cytomegalovirus (CMV) promoter into the vector for mammalian expression pcDNA3 (Invitrogen) (pcTsc). A point mutation in the EF-hand domain (D123A) as well as a silent restriction enzyme mutation (*Nsp*I) were introduced into the Tsc sequence in pET15b (pTscD123A-HisN) and pcDNA3 (pTscD123A) vectors by use of the synthetic oligonucleotide 5′-TAAAGACAAAGTGTACATACGAAGCGTCTCA-3′ and the GeneEditior site-directed mutagenesis kit (Promega). A myristoylation mutant of Tsc (pTscM2A) was constructed by PCR with a pair of synthetic oligonucleotide primers: 5′-CC**AAGCTT**ATGGCCGCTGCCCAC-3′ (with an incorporated *Hin*dIII site) and 5′-CC**GAATTC**TCAGTGGCA-GAGGGCG-3′ (with an incorporated *Eco*RI site) and cloned into the pcDNA3 mammalian expression vector. The DNA sequences of all vectors and mutations were verified by sequencing.

Expression of Wild-Type and Mutant Tsc. Hexahistidine-tagged wild-type Tsc (pTsc-HisN) or the EF-hand mutant (pTscD123A-HisN) were introduced into BL21 DE3 *Escherichia coli* cells. Cells were grown in Luria−Bertani (LB) medium (Difco) to OD_{600} 0.5, and the expression was induced by 0.4 mM IPTG for 2 h. Harvested cells were washed once with lysis buffer (50 mM sodium phosphate, 300 mM NaCl, protease inhibitor cocktail, and 10 mM imidazole, pH 7.4), and lysed in $^1/_{10}$ volume in a French pressure cell. The histidine-tagged proteins were purified on

Ni−NTA metal affinity resin as per the manufacturer's recommendation (Qiagen). Proteins were eluted with 250 mM imidazole in lysis buffer and dialyzed against 20 mM Tris and 150 mM KCl, pH 7.4. The purity of recombinant tescalcin was determined with SDS−PAGE and Coomassie staining.

Myristoylation of Tescalcin. A human tescalcin cDNA was excised as a 740 bp *Nco*I/*Pst*I fragment from pBluescript-tescalcin and cloned into *Nco*I/*Pst*I-digested pTrcHisB lacking the 5′ polyhistidine tag. BL21(DE3)pLysS *E. coli* cells were transformed with pTrc-untagged tescalcin (Amp) and pBD131(Km) for expression of tescalcin and yeast *N*-myristoyl transferase-1 (NMT-1), respectively (*21*). An overnight bacterial culture was diluted 20-fold and grown at 37 °C until OD_{600} 0.2. Recombinant protein expression and myristoylation were subsequently induced by addition of 0.5 mM IPTG and 0.1 mCi/mL [^{3}H]myristic acid, and the culture was grown for an additional 2 h at 30 °C. The bacterial cells were then harvested by centrifugation, resuspended in lysis buffer containing 20 mM Tris-HCl, pH 7.4, 100 mM NaCl, 10 mM $MgCl_2$, 1 mM dithiothreitol (DTT), 1% Triton X-100, and protease inhibitors and lysed by two rounds of freeze/thaw. The lysate was incubated with 0.1 μg/mL DNase I for 30 min on ice and cleared by centrifugation at 55000*g* for 10 min. Proteins in the supernatant were resolved by SDS−10% PAGE, and myristoylated proteins were identified by fluorography of the gel.

Gel-Filtration Chromatography. The behavior of recombinant Tsc was monitored with Superdex 75 (prep grade, Amersham Biosciences) gel-filtration chromatography. Calibration was performed with the following gel-filtration standards from Bio-Rad: thyroglobulin (670 kDa), γ-gobulin (158 kDa), ovalbumin (44 kDa), myoglobin (17 kDa), and vitamin B-12 (1.35 kDa). A 100 μL aliquot of recombinant Tsc (4 mg/mL) in 10% glycerol was passed through the column (Bio-Rad, 1.0 × 30 cm, 24 mL) in 20 mM Tris and 150 mM KCl, pH 7.4, containing either 0.5 mM $CaCl_2$, 1 mM EGTA, or 20 mM β-mercaptoethanol in 0.5 mM $CaCl_2$. Fractions were collected by drop, with each individual fraction containing 4 drops (180 μL of fluid). Each fraction was analyzed for protein concentration by measuring absorbance at 280 nm.

$^{45}Ca^{2+}$ Equilibrium Dialysis. Direct Ca^{2+}-binding measurements of Tsc were performed essentially as described by Potter et al. (*22*). Dialysis tubing with a molecular weight cutoff of 3500 (Spectra/Por, Spectrum Labs) was prepared as described in Potter et al. (*22*) to remove residual metal contaminants. Solutions of recombinant wild-type Tsc, the EF-hand mutant (D123A), parvalbumin, and soybean trypsin inhibitor were dialyzed overnight against Ca^{2+}-free buffer (10 mM MOPS, 0.1 mM EGTA, and 100 mM KCl, pH 7.0). Afterward, 0.5 mL aliquots of each of the aforementioned protein solutions (0.6−1.0 mg/mL) were dialyzed for 48−56 h at room temperature against 500 mL of the same buffer supplemented with $CaCl_2$. The amount of total $CaCl_2$ necessary to achieve a specific free Ca^{2+} concentration (pCa 7.5, 6.0, and 4.5) in the MOPS−EGTA buffering system was calculated by use of the computer program of Perrin and Sayce (*23*) and the association constant of Ca^{2+} for EGTA determined by Potter and co-workers (*24*, *25*). The amount of Ca^{2+} contamination in the water used for all experiments was determined to be $\approx 10^{-6}$ M by atomic absorption analysis. To each Ca^{2+} solution, $^{45}CaCl_2$ (Perkin-Elmer) was added to achieve approximately 13 000 cpm/50−75 μL of the 500 mL of dialysis buffer (about 60 μCi). After dialysis, three 50−75 μL aliquots of the protein solutions were dissolved in 20 mL of scintillation fluid and counted for 5 min. The concentration of each protein solution postdialysis was determined with the Coomassie Plus protein assay (Pierce). The average counts outside of the dialysis tubing were equated to the total Ca^{2+} concentration (i.e., the specific activity). Using this value, we could then determine the amount of $^{45}Ca^{2+}$ bound to each protein by subtracting the radioactivity counts within the control bag (soybean trypsin inhibitor) from the counts of the test bags (i.e., wild-type Tsc, D123A, or parvalbumin).

Intrinsic Tryptophan Fluorescence and Metal-Binding Studies. Recombinant wild-type Tsc or D123A EF-hand mutant were dialyzed extensively against 120 mM MOPS, 2 mM EGTA, and 150 mM KCl (pH 7.0). Dialysis of proteins and calculation of total $CaCl_2$ necessary to achieve a specific free Ca^{2+} concentration are described in the prior section on equilibrium dialysis. Steady-state fluorescence emission measurements were recorded at an excitation wavelength of 280 nm on an SLM-Aminco 8100 fluorescence spectrophotometer. Increasing concentrations of Ca^{2+}, Zn^{2+}, or Mg^{2+} were added to a 2 mL solution of 1 μM recombinant Tsc. Solutions were magnetically stirred for 30 s following each titration step. Average fluorescence emission values from 330 to 335 nm were obtained, corrected for dilution and then normalized ($\Delta F/\Delta F_{max}$, where F equals fluorescence). Ca^{2+} or Mg^{2+} binding curves were plotted in SigmaPlot (SPSS, Inc.), and individual affinity constants were calculated from the formula $y = (B_{max})(pCa^n)/K_d^n + pCa^n$, where B_{max} represents the maximal fluorescence change, K_d is the Ca^{2+} concentration at which tescalcin exhibits half-maximal cation binding, and n is the Hill coefficient.

Far-UV Circular Dichroism. CD spectra of 10 μM solutions of wild-type Tsc and the D123A mutant were recorded on a Jasco J-720 spectropolarimeter with a cell path length of 0.1 cm at room temperature (RT) in 5 mM Tris and 150 mM KCl, pH 7.0. Tsc protein concentrations were measured at 280 nm on the basis of the theoretical extinction coefficients (ProtParam) (*26*). Either 1 mM $CaCl_2$ or 2 mM EDTA was added, and the solutions were incubated at room temperature for 1 h to reach equilibrium. Scans were acquired from 190 to 250 nm, with a bandwidth of 1 nm, a speed of 50 nm/min, and a resolution of 0.2 nm. A total of 10 scans/sample were averaged and baselines were subtracted. Analysis and processing of data were carried out with the Jasco system software (Windows standard analysis, version 1.20). Mean residue ellipticity (θ_{MRE}, in degrees·centimeter^2·decimole^{-1}) for each spectrum was calculated from the formula $\theta_{MRE} = \theta/(10Crl)$ where θ is the measured ellipticity in millidegrees, Cr is the mean residue molar concentration, and l is the path length in centimeters. The α-helical content was calculated from an experimentally determined formula, $\theta_{MRE} = -30\,300 f_H - 2340$, where f_H is the fraction of α-helical content ($f_H \times 100$, expressed as a percentage) at 222 nm (*27*). The average spectra from two individual experiments are presented as the mean residue ellipticity and plotted in SigmaPlot.

Generation of Anti-tescalcin Antisera and Affinity Purification. A polyclonal antibody against full-length N-terminally tagged His_6-Tsc was raised in rabbits by Alpha Diagnostics International, Inc., San Antonio, TX. The antiserum was affinity-purified by passage through an Amino Link column with immobilized His_6-Tsc (Pierce).

Tissue and Cellular Lysis and Subcellular Fractionation. To study the tissue distribution of Tsc, adult mouse tissues were washed in PBS and Dounce-homogenized in lysis buffer (20 mM Tris-HCl, pH 7.6, 50 mM NaCl, 1 mM EGTA, 1 mM EDTA, and protease inhibitor cocktail). The soluble fraction was collected after centrifugation of the tissue homogenate for 30 min at 20000*g* or 100000*g* for 1 h at 4 °C. To analyze the membrane-bound fraction, the pellet was washed twice and extracted with lysis buffer supplemented with 1% Triton X-100 for 30 min on ice, followed by centrifugation for 30 min at 4 °C. Proteins (15 mg of total protein/well) were analyzed by Western blotting.

For subcellular fractionation, HeLa cells were analyzed by differential detergent extraction as described in Ramsby and Makowski (*28*). Briefly, monolayers were sequentially extracted with three detergent-containing buffers (digitonin/EDTA, Triton X-100/EDTA, and Tween-40/deoxycholate). Last, monolayers were scraped into 5% SDS and 10 mM sodium phosphate, pH 7.4, to obtain the cytoskeletal fraction. Equal protein aliquots of each lysate were analyzed by SDS−PAGE and Western blotting.

mRNA Blot. The level of expression of the Tsc gene in 76 human tissues was determined by the multiple tissue expression (MTE) array containing poly(A)+ RNAs from different human tissues and cancer cell lines. A 650 bp human Tsc cDNA fragment was labeled with ^{32}P by random priming and used as probe. The MTE array was purchased from Clontech Laboratories and the protocol used was as described in the supplied handbook.

Immunoprecipitation. Protein A−Sepharose beads were washed with 20 mM Tris and 50 mM NaCl and incubated on ice with affinity-purified anti-Tsc antibody for 1−2 h, then washed and incubated with cell or tissue extract for 1−2 h at 4 °C. After extensive washing of the beads, the bound proteins were eluted with 2× SDS−PAGE loading buffer lacking β-mercaptoethanol and analyzed by Western blotting.

Cell Culture and Transient Transfection. CHO-K1 cells were cultured in F-12K nutrient mixture Kaighn's modification (Invitrogen), PC-12 cells were cultured in F-12 (ATCC), and HeLa cells were cultured in DMEM high-glucose (Invitrogen), all of which were supplemented with 10% FBS and penicillin/streptomycin. Cells were plated in 6-well dishes 24 h prior to transfection at a concentration of 2×10^5/well for CHO-K1, PC-12, and HeLa cells. HeLa and PC-12 cells were transfected with 2 μg of pcTsc by use of LipofectAMINE reagent (Invitrogen) in OPTI-MEM medium (Gibco), and medium was replaced 5 h later. For CHO-K1 cells, 100−500 ng of pcTsc was used, with the total brought to 2 μg with empty pcDNA3. Then, 48 h after transfection, cells were washed twice with PBS, harvested in lysis buffer (20 mM Tris and 50 mM NaCl, pH. 7.6, with protease inhibitor cocktail, EDTA-free; Roche), and lysed by freeze/thaw. The soluble fraction was collected by centrifugation at 20000*g* or 100000*g* for 30 min at 4 °C.

Fluorescence Microscopy. Cells were plated onto glass coverslips and transfected 24 h later with LipofectAMINE. For PC-12 cells, coverslips were coated with poly-L-lysine. Forty-eight hours posttransfection, cells were washed twice with PBS, fixed for 25 min at RT with 3% paraformaldehyde in PBS, and permeabilized for 8 min with 0.1% Triton X-100 in PBS. Blocking was performed with 0.2% BSA in PBS for 30 min. Anti-tescalcin primary antibody was incubated at a 1:1000 dilution for 1 h and then with anti-rabbit fluorescein-conjugated secondary IgG (AP Biotech) at a 1:400 dilution for 30 min along with Hoechst (2 μg/mL). For colocalization studies, slides were incubated with the anti-tescalcin antibody along with either the nucleoporin mouse antibody mAB414 (provided by Beatriz Fontoura, University of Miami) or mouse anti-Rac1 1:200 (Upstate) for 1 h. Anti-mouse Cy3-conjugated secondary IgGs were used at a concentration of 1:200 for 30 min (Jackson ImmunoResearch). After incubation with secondary antibodies, cells were washed three times for a total of 15 min, mounted on glass slides with ProLong mounting medium (Molecular Probes, Inc.), and observed under phase and fluorescence microscopy (Nikon Eclipse TE2000-U microscope). Confocal images were obtained with a Zeiss LSM-510 microscope.

Calcineurin Phosphatase Assay. Wild-type Tsc or the D123A mutant (8 μM) was added to recombinant CnA and CnB (40 units) in the absence or presence of 0.25 μM CaM and preincubated for 10 min at 30 °C. Phosphorylation buffer consisted of 100 mM Tris, pH 7.5, 200 mM NaCl, 12 mM $MgCl_2$, 1 mM dithiothreitol, 0.05% NP-40, and 1 mM $CaCl_2$, and tescalcin was in 5 mM Tris and 50 mM NaCl, pH 7.4. Subsequently, 45 μM of a synthetic phosphorylated peptide substrate (Asp-Val-Pro-Ile-Pro-Gly-Arg-Phe-Asp-Arg-Val-pSer-Val-Ala-Ala-Glu) was added and further incubated for 30 min at 30 °C. Afterward, malachite green was rapidly added to halt the reaction, and the level of free phosphate released was analyzed by measuring the absorbance at 630 nm. All reagents were purchased from Biomol Research Laboratories as part of the calcineurin assay kit. The data were normalized to the amount of free phosphate released by calcineurin plus CaM in buffer alone. Soybean trypsin inhibitor, STI, was used as a negative control since this protein has a similar molecular weight and p*I* as tescalcin. As a positive control, a final concentration of 40 μM calcineurin autoinhibitory peptide was used (Ile-Thr-Ser-Phe-Glu-Glu-Ala-Lys-Gly-Leu-Asp-Arg-Ile-Asn-Glu-Arg-Met-Pro-Pr o-Arg-Arg-Asp-Ala-Met-Pro); this peptide mimics the region in CnA that is involved in autoinhibition (Biomol) (*29*).

RESULTS

Sequence Analysis of Tescalcin. The amino acid sequences of human and mouse tescalcin are highly homologous (96% identity, 99% similarity), both possessing an N-terminal myristoylation motif and predicted molecular mass of 24.5 kDa. Tescalcin shares significant sequence homology with three other 19−22 kDa EF-hand Ca^{2+}-binding proteins: CHP1 (calcineurin homologous protein, also known as p22) (34% identity, 54% similarity), CHP2 (also known as hepatocellular carcinoma-associated antigen 520) (29% identity, 48% similarity), and calcineurin B (27% identity, 50% similarity), as presented in Figure 1. The CnB sequence

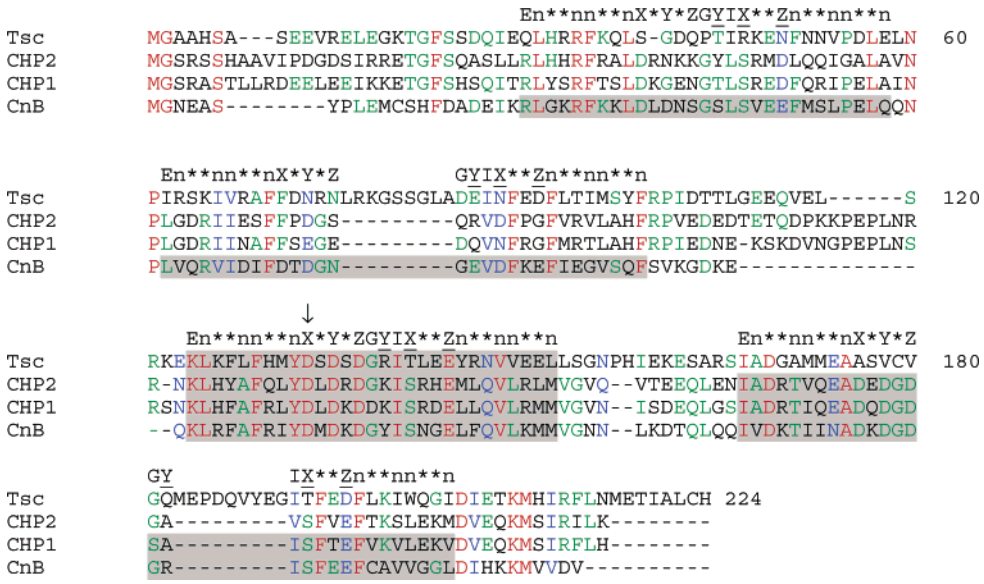

FIGURE 1: Sequence alignment of tescalcin with CHP1 and 2 and calcineurin B. By use of Multalin software (*49*), the amino acid sequences of the following four proteins were aligned: tescalcin (*Mus musculis*, GenBank Accession No. AAH19492); CHP1 (*Rattus norvegicus*, Q62877), CHP2 (*Homo sapiens*, NM022097), and CnB (*Rattus norvegicus*, L03554). EF-hands are highlighted in gray; the tescalcin (Tsc), calcineurin homologous protein (CHP1,2), and calcineurin B (CnB) sequences contain one, two, and four consensus EF-hands, respectively. Tsc and/or CHP may also contain additional ancestral EF-hands. The consensus EF-hand domain consists of a 29 amino acid long helix−loop−helix array (En**nn**nX*Y*ZGYIX**Zn**nn**n). A Ca^{2+} ion is coordinated by oxygen in the side chains of amino acids X, Y, Z and from a water molecule hydrogen-bonded to residue (X) (*30*). The most common amino acids that bind Ca^{2+} at the X, Y, and Z positions include serine (S), aspartate (D), and asparagine (N). The residue at position Y donates a carbonyl oxygen and can be any amino acid, whereas the residue at position Z (glutamate or aspartate) binds Ca^{2+} with two oxygen atoms. The glycine at position G permits a bend in the EF-hand loop, and a hydrophobic residue (leucine, isoleucine, or valine) is present at position I (*30*). The two neighboring α-helices contain alternating hydrophilic (*) and hydrophobic (n) residues. The arrow indicates the aspartate at position X of the tescalcin EF-hand loop that was mutated to alanine to obtain a Ca^{2+}-binding-deficient mutant (D123A).

has four EF-hand regions and binds four Ca^{2+} ions. CHP1 and CHP2 are described in the literature to have only two EF-hand regions, although it is likely that there are two other helix−loop−helix regions. Tescalcin has only one true consensus EF-hand domain that is recognized by BLAST searching. This EF-hand spans residues 114−142 near the C-terminus of tescalcin and aligns to the third EF-hand of CnB (EF3). The alignment of tescalcin with the sequences of CnB and CHP also reveal probable remnants of ancestral EF-hand domains within the tescalcin sequence, regions that retain the helix−loop−helix structure but may fail to coordinate Ca^{2+} ions. The regions in the tescalcin sequence that align with EF2 and EF4 of CnB deviate from the consensus EF-hand sequence due to amino acid insertions that may prevent the formation of an EF-hand structure. A region in tescalcin that corresponds to CnB's EF1 has amino acid substitutions in place of critical Ca^{2+}-binding residues, including glycine, arginine, and asparagine at positions Y, X, and Z, respectively. Tescalcin's EF1 also has a proline instead of a glycine, which may perturb the EF-hand "loop" (*30*). Since only a handful of EF-hand proteins bind a single Ca^{2+} ion (*31*), it is of interest to analyze the metal binding characteristics of tescalcin and delineate the important site(s), especially whether binding is achieved via the true consensus EF-hand or whether the other three ancestral EF-hands retain their Ca^{2+}-binding function.

Purification of Recombinant Tescalcin. Recombinant N-terminally hexahistidine-tagged mouse tescalcin was obtained as soluble protein with a yield of about 50 mg/L of *E. coli* culture (Figure 2A). Under denaturing conditions, His_6-tagged tescalcin runs at approximately 27 kDa in SDS−PAGE. When coexpressed in *E. coli* along with yeast *N*-myristoyl transferase-1, human untagged tescalcin was specifically labeled with [^{3}H]myristic acid, showing that tescalcin can be N-myristoylated (Figure 2B). We observed tescalcin dimers in vitro in native PAGE (Figure 2C), which apparently results, at least in part, from disulfide formation, as the amount of the dimeric form of tescalcin is decreased by addition of β-mercaptoethanol. Superdex 75 gel-filtration chromatography of recombinant tescalcin in the presence or absence of 20 mM β-mercaptoethanol in 0.5 mM Ca^{2+} confirmed these results, illustrating that the dimeric form of tescalcin represents about 10% of the total protein content (Figure 2D). This ratio is not altered by 1 mM EGTA (data not shown). The presence of the dimeric and monomeric forms of tescalcin in chromatography fractions was confirmed by Coomassie staining and Western blotting (Figure 2E,F). Interestingly, although the dimeric form appears to be stable, a small fraction of the monomer seems to spontaneously dimerize postchromatography (Figure 2F). In contrast to some other EF-hand proteins, the electrophoretic mobility of tescalcin does not change in the presence or absence of Ca^{2+} (data not shown).

Direct $^{45}Ca^{2+}$ Binding Analysis with Equilibrium Dialysis. Although tescalcin has several putative EF-hands, it is unclear whether it binds Ca^{2+} ions, and if so, how many. A third of known EF-hand motifs fail to bind Ca^{2+} and may instead bind Mg^{2+} with low affinity (*30*). Using equilibrium dialysis as discussed by Potter et al. (*22*), we monitored the stoichiometry of Ca^{2+} binding at physiologically relevant Ca^{2+} concentrations. At free calcium concentrations less than pCa 4.5, tescalcin binds $^{45}Ca^{2+}$ with a stoichiometry of 0.69 ± 0.06 mol of Ca^{2+}/mol of protein, while parvalbumin, our positive control with two Ca^{2+}-binding sites, binds 1.8 ±

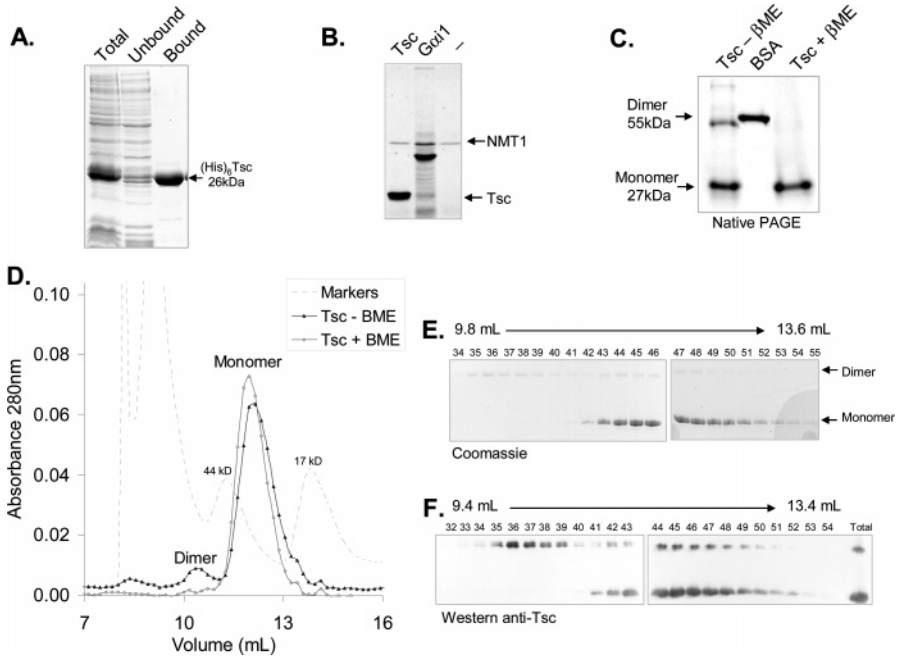

FIGURE 2: Purification of recombinant tescalcin, formation of disulfide dimers, and N-myristoylation in vitro. (A) N-terminally His_6-tagged recombinant mouse Tsc was purified from the soluble fraction of *E. coli* lysate by nickel-NTA−agarose chromatography. The purity of Tsc was determined with SDS−PAGE followed by Coomassie staining. (B) Human untagged Tsc (left lane) or $G\alpha_{i1}$ (positive control, middle lane) were expressed in *E. coli* with yeast *N*-myristoyl transferase-1 (NMT-1), whereas in the right lane only NMT-1 was expressed. The bacterial cells were grown in medium containing 0.5 mM isopropyl β-D-1-thiogalactopyranoside and 0.1 mCi/mL [^{3}H]myristic acid for 2 h at 30 °C. Cells were harvested and resolved on an SDS−10% polyacrylamide gel. Myristoylated proteins were identified by detecting radiolabeled protein bands by fluorography. (C) Native PAGE in the absence of SDS was performed on recombinant mouse His_6-Tsc in the presence or absence of β-mercaptoethanol, with BSA (middle lane) as the protein standard. (D) Recombinant tescalcin (4 mg/mL) was resolved by Superdex 75 gel-filtration chromatography in 20 mM Tris, 150 mM KCl, pH 7.4, and 0.5 mM $CaCl_2$ in the presence or absence of 20 mM β-mercaptoethanol (β-ME). The column was calibrated with the following gel-filtration standards as depicted by the gray dashed line: thyroglobulin (670 kDa), γ-gobulin (158 kDa), ovalbumin (44 kDa), myoglobin (17 kDa), and vitamin B-12 (1.35 kDa). Fractions were collected by drop, with each fraction containing 4 drops, or 180 μL. (E) Analysis of column fractions by Coomassie staining. The dimer (elution volume 10.4 mL) was separated from the monomer (elution volume 12 mL). It appears that a small fraction of the monomeric form has spontaneously dimerized following the chromatography. (F) Western blot analysis of column fractions with tescalcin antibody. The ratio of the dimer with respect to the monomer appears to be higher in the Western blot than in the Coomassie due to saturation of the ECL signal in fractions containing the monomer.

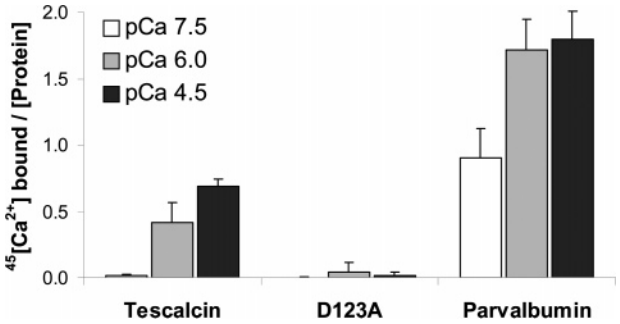

FIGURE 3: Equilibrium dialysis of tescalcin and EF-hand mutant. Wild-type tescalcin, the D123A mutant, and parvalbumin (0.6−1 mg/mL) were dialyzed extensively for 48−56 h against solutions containing several different free Ca^{2+} concentrations (pCa 7.5, 6.0, and 4.5) in 10 mM MOPS, 100 mM KCl, 0.1 mM EGTA, pH 7.0, and 60 μCi of $^{45}CaCl_2$. The stoichiometry of $^{45}Ca^{2+}$ binding was determined as described under Experimental Procedures. Values represent the average and standard deviation of three independent experiments. At pCa 4.5, tescalcin binds $^{45}Ca^{2+}$ with a stoichiometry of 0.69 ± 0.06 mol of Ca^{2+}/mol of protein, while parvalbumin, our positive control with two Ca^{2+}-binding sites, binds 1.8 ± 0.2 mol of Ca^{2+}/mol of protein. In contrast, the D123A mutant of tescalcin binds 0.02 ± 0.02 mol of Ca^{2+}/mol of protein.

0.2 mol of Ca^{2+}/mol of protein, which is close to the theoretical value of 2 mol/mol (Figure 3). To establish that the Ca^{2+}-binding site was indeed within the single EF-hand spanning residues 114−142 and not another atypical EF-hand, we replaced the Asp at position X of the EF-hand with Ala (D123A), as shown by the arrow in Figure 1. This residue is the first amino acid of the EF-hand loop to coordinate Ca^{2+} (*32*). This D123A mutation abolished $^{45}Ca^{2+}$ binding (binding was near zero: 0.02 ± 0.02 mol of Ca^{2+}/mol of protein) (Figure 3). Hence, in physiological conditions, tescalcin is expected to bind one Ca^{2+} ion via the third EF-hand.

Effect of Divalent Cations on Tescalcin Intrinsic Tryptophan Fluorescence. We next monitored tescalcin's conformational change by intrinsic fluorescence spectrophotometry of the single tryptophan residue (Trp-191) near the C-terminus. Tescalcin displayed a large decrease in tryptophan fluorescence with increasing concentrations of Ca^{2+}, with minimal shift in the emission maximum (Figure 4A,B). This reveals that Trp-191 is within a region of the protein undergoing a Ca^{2+}-dependent conformation change. Quenching of fluorescence by Ca^{2+} has also been found in several other EF-hand Ca^{2+}-binding proteins and may result from a decrease in the hydrophobicity of the environment surrounding the tryptophan residue (*33*−*36*). By Ca^{2+} titration, we calculated the K_d of tescalcin for Ca^{2+} as 810 nM (SD 50 nM); the Hill coefficient was found to be 1.2 (Figure 4C). Tescalcin fails to exhibit a fluorescence change with Zn^{2+}, indicating the conformational change caused by Ca^{2+} binding is specific and not from nonspecific divalent cation effects.

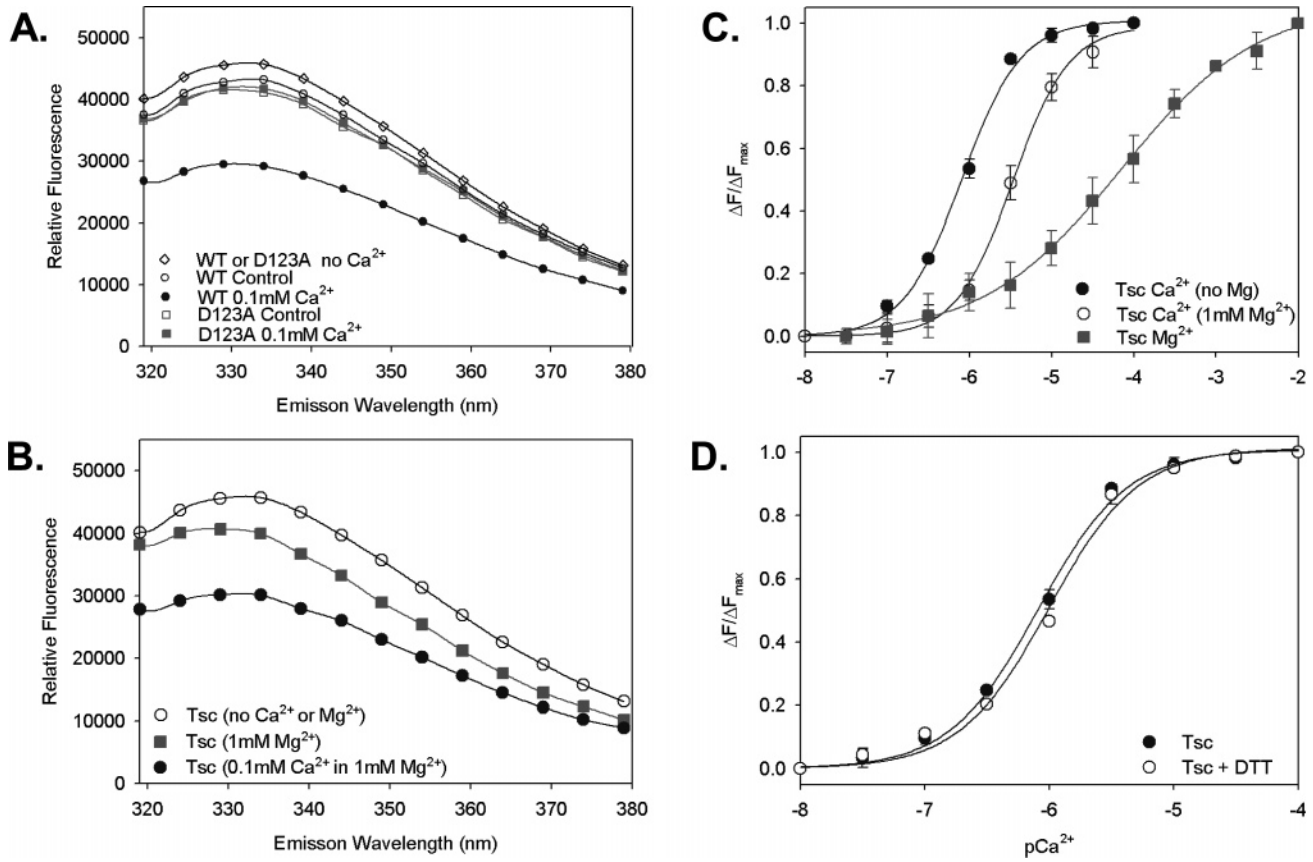

FIGURE 4: Ca^{2+}- and Mg^{2+}-mediated changes in the intrinsic tryptophan-191 fluorescence of tescalcin. Recombinant His_6-tescalcin was dialyzed into 120 mM MOPS containing 2 mM EGTA and 150 mM KCl (pH 7.0), and steady-state fluorescence measurements were performed with an excitation wavelength of 280 nm. (A) Spectra of 1 μM wild-type (WT) tescalcin in the absence of Ca^{2+} (◇) or after titration with control (H_2O, ○) or 1 mM Ca^{2+} (●). Also shown are spectra of 1 μM EF-hand mutant (D123A) in the absence of Ca^{2+} (◇) or after titration with control (H_2O, □) or 0.1 mM Ca^{2+} (■). The EF-hand mutant fails to exhibit a Ca^{2+}-induced conformational change; its fluorescence spectrum does not vary significantly from the control (addition of water). (B) Spectra of 1 μM tescalcin without added cations (○), in the presence of 1 mM Mg^{2+} (■), and with 0.1 mM Ca^{2+} in the presence of 1 mM Mg^{2+} (●). Three to six independent experiments were performed for each curve. (C) Tescalcin dose-dependent binding to Ca^{2+} ions (●), Ca^{2+} in the presence of 1 mM Mg^{2+} ions (○), and Mg^{2+} alone (■). The Hill coefficient for Ca^{2+} binding is 1.2, whereas for Mg^{2+} it is 0.5. (D) In the presence of 1 mM dithiothreitol (DTT), the Ca^{2+} affinity of tescalcin is not changed (○). The error bars represent the standard deviation of each point.

Tescalcin's Ca^{2+} affinity is not altered by the addition of DTT (Figure 4D).

Figure 3 shows that the D123A mutation completely abolishes the Ca^{2+}-induced fluorescence change, which provides evidence that the EF-hand spanning residues 114−142 is alone responsible for the Ca^{2+}-dependent rearrangement in protein structure. It is of interest to note that this D123A mutant, when transiently transfected in CHO-K1 cells, was detected at much lower levels than wild-type tescalcin (see Figure 6D), suggesting that the Ca^{2+}-bound conformation may increase the protein's stability in mammalian cells.

Using intrinsic tryptophan fluorescence, we also found that tescalcin can bind Mg^{2+} ions. The Mg^{2+}-induced fluorescence decrease is much smaller than with Ca^{2+} and is accompanied by a 3 nm blue shift in emission wavelength (Figure 4A). The calculated affinity of tescalcin for Mg^{2+} is 73 μM (SD 32 μM); the Hill coefficient is 0.5 (Figure 4C). The broad curve and negative Hill slope may indicate that, at high concentrations, Mg^{2+} binds to more than one site. Mg^{2+} clearly affects Ca^{2+} binding: in the presence of 1 mM Mg^{2+}, the affinity of tescalcin for Ca^{2+} is shifted to 3.5 μM (SD 0.7 μM). Since physiological Mg^{2+} concentrations are within the millimolar range (*30*), these results suggest that in a living cell tescalcin constitutively binds Mg^{2+}, but during the momentary increases of intracellular Ca^{2+} upon stimulation, Mg^{2+} may be exchanged for Ca^{2+} ions.

Circular Dichroism of Tescalcin and EF-Hand Mutant. Since many proteins of the EF-hand superfamily undergo a Ca^{2+}-induced change of secondary structure, we obtained far-UV circular dichroic spectra for the wild type and D123A EF-hand tescalcin mutant. Wild-type tescalcin displayed a very small but reproducible decrease in the mean residue ellipticity (205−225 nm) upon addition of Ca^{2+} (Figure 5A). This difference translated into a change in overall secondary structure from 21.6% α-helical content in 2 mM EDTA to 22.4% with 1 mM $CaCl_2$ (Figure 5C). Since the change was so small, we could not determine the half-maximal Ca^{2+} concentration at which it occurred. The secondary structure of the EF-hand mutant was similar to that of the wild type, showing that, as expected, the D123A point mutation did not significantly perturb the secondary structure of tescalcin (Figure 5B). In contrast to the wild-type tescalcin, this mutant failed to show even a small Ca^{2+}-induced change in its circular dichroic spectrum.

Production and Purification of Anti-tescalcin Antibodies. We raised rabbit polyclonal antibodies against the full-length N-terminally His_6-tagged recombinant tescalcin. After affinity

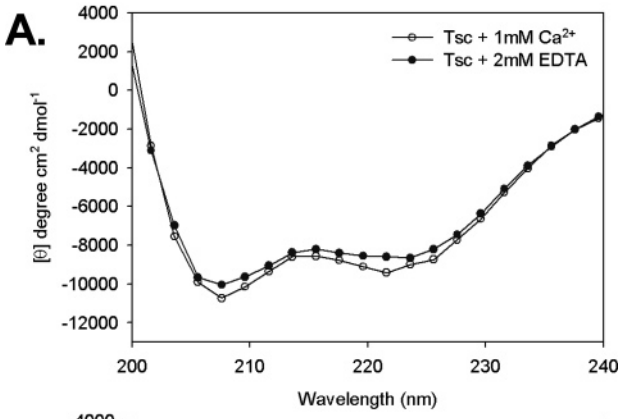

C.

Condition	$[\theta]_{222}$	α-helical content
Tsc Ca^{2+}	-9133	22.4%
Tsc EDTA	-8869	21.5%
D123A Ca^{2+}	-8401	20.0%
D123A EDTA	-8471	20.2%

FIGURE 5: Far-UV circular dichroism reveals small Ca^{2+}-induced change in secondary structure of wild-type tescalcin but not the EF-hand mutant. Recombinant wild-type or D123A tescalcin (10 μM) was analyzed by circular dichroism as discussed under Experimental Procedures. (A) Mean residue ellipticity (θ, in degrees·centimeter^2·decimole^{-1}) versus wavelength of wild-type tescalcin in the presence of either 1 mM Ca^{2+} (○) or 2 mM EDTA (●) in 5 mM Tris and 150 mM KCl, pH 7.0 ($n = 2$). (B) Spectra of D123A mutant in 1 mM $CaCl_2$ (□) and 2 mM EDTA (■). (C) Average values of θ_{MRE} (mean residue ellipticity in degrees·centimeter^2·decimole^{-1}) and f_H (fraction of α-helical content) of wild-type and D123A tescalcin at 222 nm ($n = 2$).

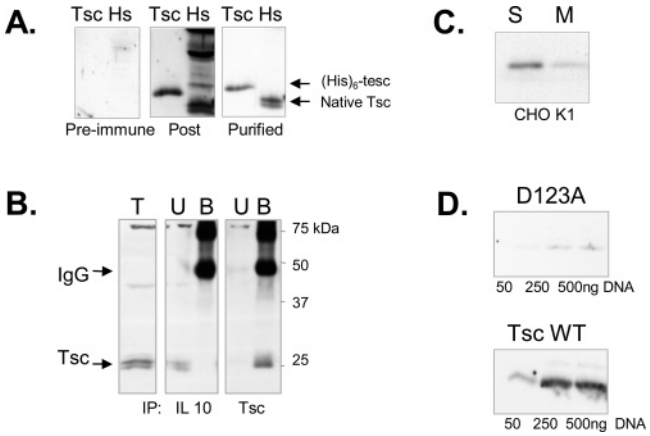

FIGURE 6: Characterization of anti-tescalcin antibody and tescalcin in cultured cells. To facilitate analysis of tescalcin protein expression and localization, an antibody was raised in rabbits against full-length His_6-tagged mouse tescalcin. (A) Affinity purification of anti-tescalcin rabbit antibody by use of immobilized recombinant tescalcin. Western blotting on recombinant His_6-tescalcin (Tsc) and the soluble fraction of mouse heart tissue (Hs) was performed with preimmune rabbit serum, postimmunization anti-tescalcin rabbit serum, and affinity-purified serum. (B) Immunoprecipitation with anti-Tsc or anti-IL-10 (negative control) antibodies of stomach lysate was performed as described under Experimental Procedures. Fractions from the immunoprecipitation were analyzed by Western blotting with the anti-tescalcin antibody (total lysate, T; unbound, U; and bound, B). (C) Presence of tescalcin in soluble (S) and membrane (M) fractions of CHO-K1 cells transiently overexpressing tescalcin. (D) Levels of ectopic wild-type tescalcin and the EF-hand mutant (D123A) in CHO-K1 cells with increasing concentration (50−500 ng) of the plasmid expressing tescalcin (pcTsc or pTscD123A).

purification on immobilized tescalcin, the antibody detects nanogram quantities of the recombinant protein (Figure 6A). In tissues and cell lines, it recognizes a band at 24 kDa (Figure 6A), which is close to the calculated theoretical molecular weight of tescalcin. This protein can be immunoprecipitated with our antibody from mouse heart, brain, and stomach lysates as well as when overexpressed in CHO-K1 cells (Figure 6B). In addition to tescalcin, the antibody recognizes two bands with apparent masses of approximately 40 and 75 kDa. In contrast to the 24 kDa tescalcin band, these proteins could not be immunoprecipitated, and hence we attribute them to nonspecific staining. Our antibody also detects ectopically expressed tescalcin in CHO-K1 cells as well as endogenous tescalcin in HeLa cells with a molecular mass of 24 kDa (Figures 6C and 7C). A faint tescalcin band is detected in the 100000*g* supernatant of HeLa cells, while upon overexpression in CHO-K1 or HeLa cells, some tescalcin is detected in membrane/particulate fractions (data not shown). As mentioned earlier, WT tescalcin was expressed readily, whereas the D123A mutation reduced the protein levels (Figure 6D).

Tescalcin mRNA and Protein Expression in Tissues and Cell Lines. Previously, our Northern blot analysis of mRNA from adult mouse tissues demonstrated a high level of tescalcin expression in the heart with weaker expression in the brain and kidney. Although no tescalcin mRNA was found in the adult testis with Northern analysis, mRNA was detected by RT-PCR (*1*). Our results differed from the study by Mailander et al. (*19*), which found tescalcin mRNA solely in the heart. In the present study, by RNA blotting and protein immunoblotting, we demonstrate that tescalcin's mRNA and protein expression in mouse tissues is in agreement with our previous data (*1*).

In a human mRNA array blot, we found that tescalcin mRNA is highly expressed in the heart (atrium, ventricle, septum, and apex) and stomach (duodenum) (Figure 7A). In the brain, tescalcin mRNA is most abundant in the caudate-putamen but low in the cerebellum and medulla. Tescalcin is also abundant in salivary gland, bone marrow, pancreas, and adrenal glands but is expressed at low to undetectable levels in adult lung, placenta, ileum, kidney, skeletal muscle, spleen, thymus, and lymph node. While expressed at moderate levels in the adult testis and prostate, mRNA levels are quite low in the ovary, uterus, and mammary gland. Interestingly, tescalcin expression is much

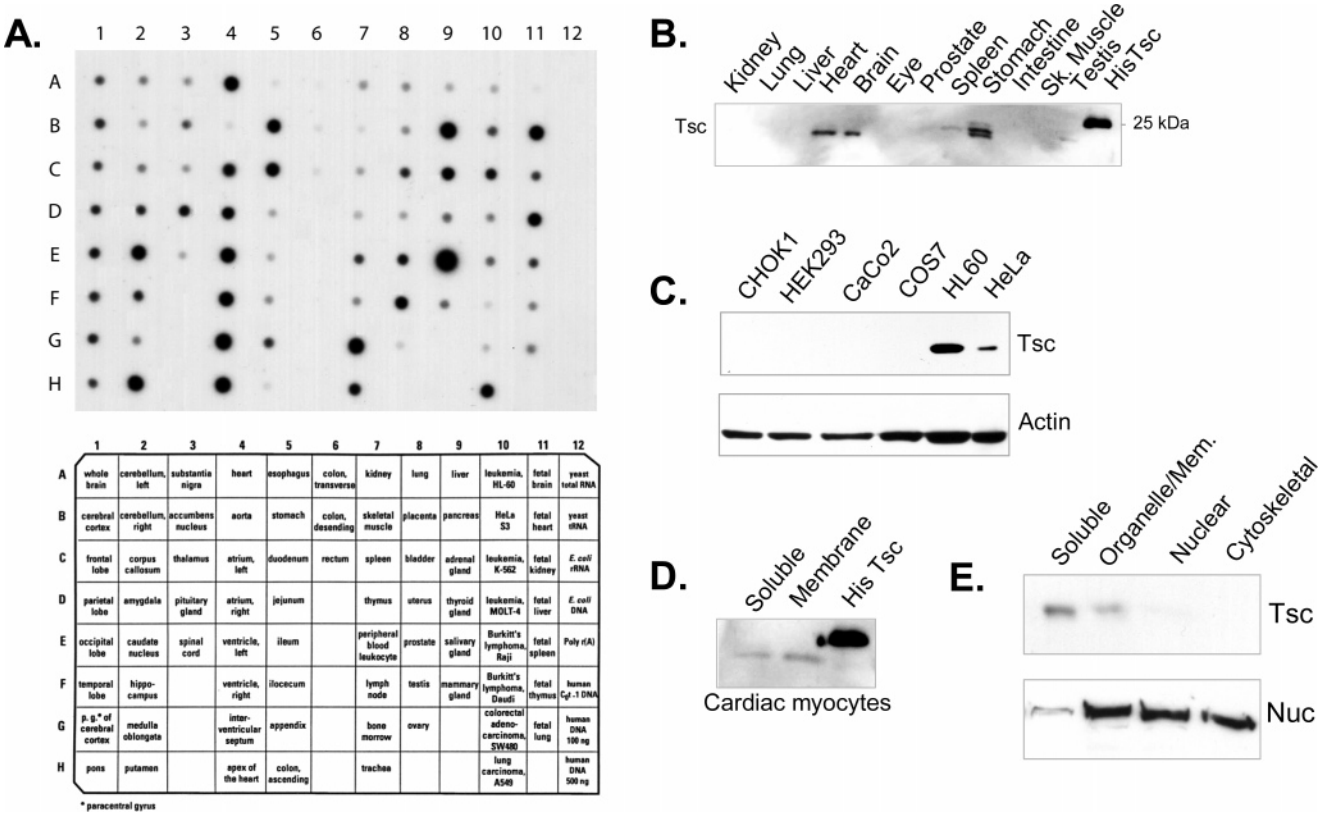

	1	2	3	4	5	6	7	8	9	10	11	12
A	whole brain	cerebellum, left	substantia nigra	heart	esophagus	colon, transverse	kidney	lung	liver	leukemia, HL-60	fetal brain	yeast total RNA
B	cerebral cortex	cerebellum, right	accumbens nucleus	aorta	stomach	colon, descending	skeletal muscle	placenta	pancreas	HeLa S3	fetal heart	yeast tRNA
C	frontal lobe	corpus callosum	thalamus	atrium, left	duodenum	rectum	spleen	bladder	adrenal gland	leukemia, K-562	fetal kidney	*E. coli* rRNA
D	parietal lobe	amygdala	pituitary gland	atrium, right	jejunum		thymus	uterus	thyroid gland	leukemia, MOLT-4	fetal liver	*E. coli* DNA
E	occipital lobe	caudate nucleus	spinal cord	ventricle, left	ileum		peripheral blood leukocyte	prostate	salivary gland	Burkitt's lymphoma, Raji	fetal spleen	Poly r(A)
F	temporal lobe	hippo-campus		ventricle, right	ilocecum		lymph node	testis	mammary gland	Burkitt's lymphoma, Daudi	fetal thymus	human C_0t -1 DNA
G	p. g.* of cerebral cortex	medulla oblongata		inter-ventricular septum	appendix		bone marrow	ovary		colorectal adeno-carcinoma, SW480	fetal lung	human DNA 100 ng
H	pons	putamen		apex of the heart	colon, ascending		trachea			lung carcinoma, A549		human DNA 500 ng

* paracentral gyrus

FIGURE 7: Tescalcin has a restricted mRNA and protein expression pattern in mouse tissues and cell lines. (A) A multiple tissue expression mRNA array (Clontech) was probed with ^{32}P-labeled human tescalcin cDNA. High levels of expression were observed in the heart, stomach, duodenum, bone marrow, testes, pancreas, adrenal gland, salivary gland, and fetal liver. The bottom panel describes the origin of the poly(A)+ RNA present in the corresponding regions of the top panel. (B) Western blots showing the expression of tescalcin protein in the soluble fraction of various adult mouse tissues, 15 μg of protein/lane. (C) Tescalcin protein expression in multiple normal and cancer cell lines, 20 μg of protein/lane. (D) Immunoblotting of tescalcin in the soluble and membrane fractions from mouse neonatal cardiac myocytes, 15 μg of protein/lane. (E) Subcellular fractionation by differential detergent extraction of endogenous tescalcin from HeLa cells into the following fractions: cytosolic, organelle/membrane, nuclear, and cytoskeletal. Fractionation was also monitored by Western blotting with anti-nucleolin antibody.

higher in fetal liver and kidney when compared to the adult, whereas fetal brain shows very low expression. In the lung carcinoma cell line A549, tescalcin shows an aberrant high mRNA expression, although expression levels are low in normal adult lung. Other cell lines expressing tescalcin mRNA include the cervical cancer line HeLa and the human myeloid leukemia cell lines HL-60 and K562.

Through immunoblot analysis of adult mouse tissues, we provide conclusive evidence that the tescalcin gene encodes a 24 kDa protein that is most abundant in the adult mouse stomach, heart, and brain (Figure 7B). Tescalcin is detected as a single band in Western blots of heart and brain extracts and as a doublet in stomach. This doublet may result from alternative splicing, proteolysis, or posttranslational modifications. Although a small amount of tescalcin remains in the particulate fraction, the majority (50−80%) is found in the 100000*g* supernatant. Tescalcin is also expressed at minor levels in the adult spleen, kidney, and testis and is undetectable in mouse eye, colon, lung, and skeletal muscle (Figure 7B). Tescalcin protein is highly expressed in cultured neonatal cardiac myocytes and the cancer cell lines HeLa and HL-60. Low to undetectable expression is seen in COS-7, CaCo-2, CHO-K1, PC-12, and HEK-293 cells (Figure 7C,D). Detection in human cell lines (HeLa and HL-60) reveals the cross-reactivity of our antibody with the human form of tescalcin. We also performed subcellular fractionation of endogenous tescalcin in HeLa cells by two methods. The first method, described by Ramsby and Makowski (*28*), uses different detergents to differentiate between cytoplasmic, organelle/membrane, nuclear, and cytoskeletal fractions, and we show that tescalcin is detected predominantly in the cytoplasmic and organelle/membrane fractions (Figure 7E). We also detected tescalcin primarily in the soluble pool and minor amounts in the nuclear fraction after isolation of HeLa nuclei by detergent extraction with 0.5% NP-40 and centrifugation for 5 min at 800*g* (data not shown).

Subcellular Localization of Tescalcin. Immunostaining of CHO-K1 and PC-12 cells transiently transfected with tescalcin cDNA revealed diffuse cytosolic and nuclear staining, which is characteristic of a small protein that can diffuse through nuclear pores (Figure 8A−D). Tescalcin appears to be concentrated in the region around the nucleus, as revealed by double immunostaining with antibody for the nuclear pore complex, mAb414 (Figure 8D). Many other EF-hand proteins are also found to be perinuclear, including CHP1 (*17*). Tescalcin is also localized to membrane regions corresponding to lamellipodia and membrane ruffles in CHO-K1 and HeLa cells, where it colocalizes with the marker small GTPase Rac-1 (Figure 9B); this membrane staining corroborates our data demonstrating a small percentage of tescalcin in membrane fractions (Figure 7E). Tescalcin localization to lamellipodia and membrane ruffles is decreased upon serum starvation (Figure 9A); Rac-1 is also absent from these membrane regions during serum star-

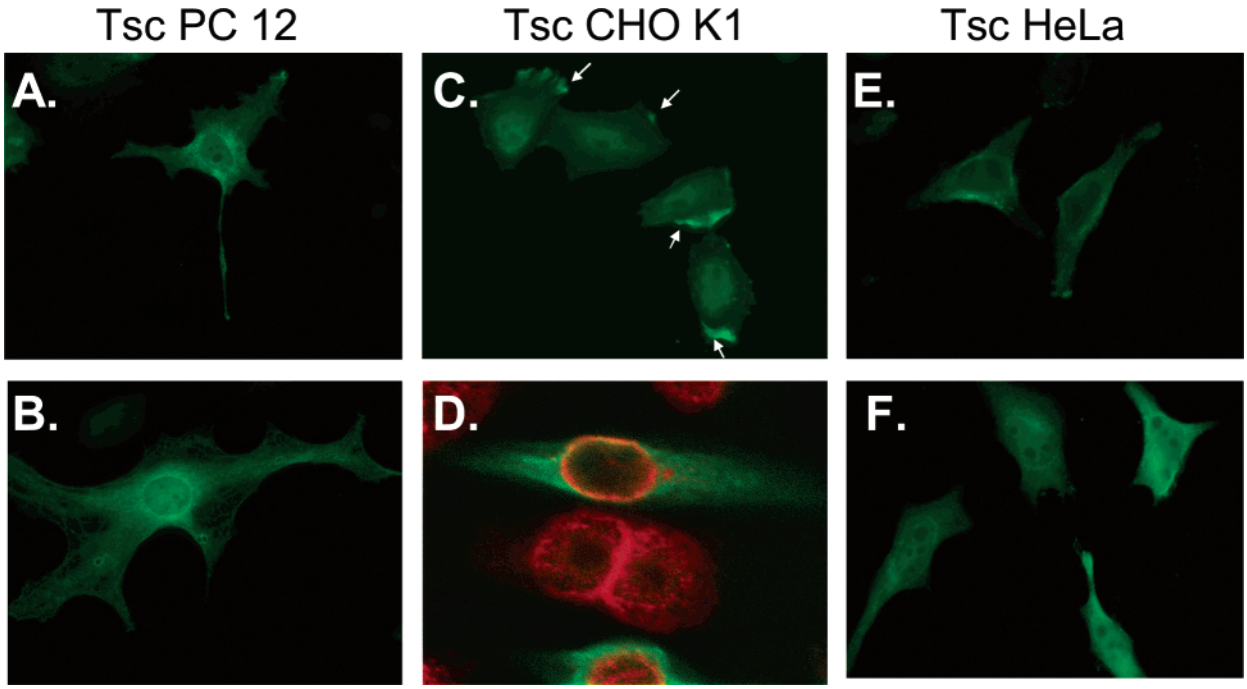

FIGURE 8: Subcellular localization of tescalcin in several cell lines. PC-12 (A, B), CHO-K1 (C), and HeLa (E, F) cells were transiently transfected with tescalcin cDNA for 48 h, fixed with 3% paraformaldehyde, and stained with rabbit tescalcin primary antibody and fluorescein-conjugated secondary antibody. Imaging was performed by fluorescence microscopy (Nikon Eclipse TE2000-U microscope). (D) Confocal image of tescalcin (green) and mAb414 for nucleoporins (red) in CHO-K1 cells overexpressing tescalcin, obtained with a Zeiss LSM-510 microscope.

vation. It is noteworthy that human tescalcin and NHE are also enriched in lamellipodia (*19*, *37*). In HeLa cells, overexpressed tescalcin is found in the cytosol and perinuclear region (Figure 8E,F) and in lamellipodia induced with introduction of constitutively active Rac-1 (data not shown).

We did not observe a localization shift in response to alterations of intracellular Ca^{2+} levels by BAPTA-AM, ionomycin, or thapsigargin incubation (data not shown). Furthermore, the tescalcin EF-hand mutant (D123A) deficient in Ca^{2+} binding exhibited a similar cytosolic localization pattern with concentration at lamellipodia, as observed for wild-type tescalcin. Thus, it appears that Ca^{2+} binding does not alter tescalcin localization to a significant degree. A mutation of the glycine residue at position 2 for an alanine, which prevents N-myristoylation, also did not have a visible effect on localization.

Effect of Tescalcin on Calcineurin Phosphatase Activity. Since tescalcin shares 50% amino acid similarity with calcineurin B and CHP (calcineurin homologous protein), we tested the hypothesis that tescalcin's similarity to CHP may endow it with similar effects on calcineurin activity. We therefore tested the effect of recombinant tescalcin on the activity of calmodulin-stimulated calcineurin in a colorimetric assay. The results shown in Figure 10 demonstrate that tescalcin inhibits the amount of phosphatase released by CaM-stimulated CnA to 56.8% ± 0.6% of the maximal value. This effect is comparable to the inhibition by the positive control, a peptide resembling the autoinhibitory domain of CnA, 55% ± 6% (*9*). There was no effect of tescalcin on calcineurin activity in the absence of CaM. We found that the D123A EF-hand mutant also inhibits calcineurin activity, indicating that CnA inhibition does not depend on Ca^{2+} binding.

DISCUSSION

Tissue Distribution and Subcellular Localization of Tescalcin. Our previous study revealed that tescalcin mRNA is preferentially expressed in the developing mouse testis as determined by representational difference analysis at 13.5 dpc (*1*). By in situ hybridization of testis tissue, the mRNA was found to be restricted to the developing sex cords. In this study, we demonstrate the existence of the tescalcin gene product in various mouse and human tissues along with several cancerous cell lines. Although tescalcin was originally named for the discovery of its mRNA expression in the embryonic testis, in the adult mouse we show that the protein is actually most abundant in the stomach, heart, and brain, with minor expression in adult testis (Figure 7B). This tissue expression pattern differs significantly from tescalcin's homologues , CHP-1 and calcineurin B, which are expressed ubiquitously, and CHP2, which is detected only in cancerous tissue (*8*−*10*). Interestingly, certain isoforms of CnA and CnB are enriched in the testis (*38*). Calcineurin A is a major constituent of brain and, like tescalcin, has higher expression in the caudate and hippocampus (*39*).

The fact that tescalcin expression is abundant in tissues other than the testis signifies that tescalcin has a role in adult cellular Ca^{2+} signaling and homeostasis in addition to a role in embryonic testis development. Expression in the stomach is interesting in light of the fact that the NHE subtypes are important for cell volume regulation and intracellular pH (*17*). Since tescalcin is also expressed in the brain, it is likely that tescalcin plays a neurospecific role, especially given the fact that tescalcin bears an N-myristoylation motif and has a Ca^{2+} affinity similar to other neuronal Ca^{2+}-binding proteins (Figures 2B and 4C) (*40*). N-myristoylation of tescalcin may impart a Ca^{2+}-induced myristoyl switch that

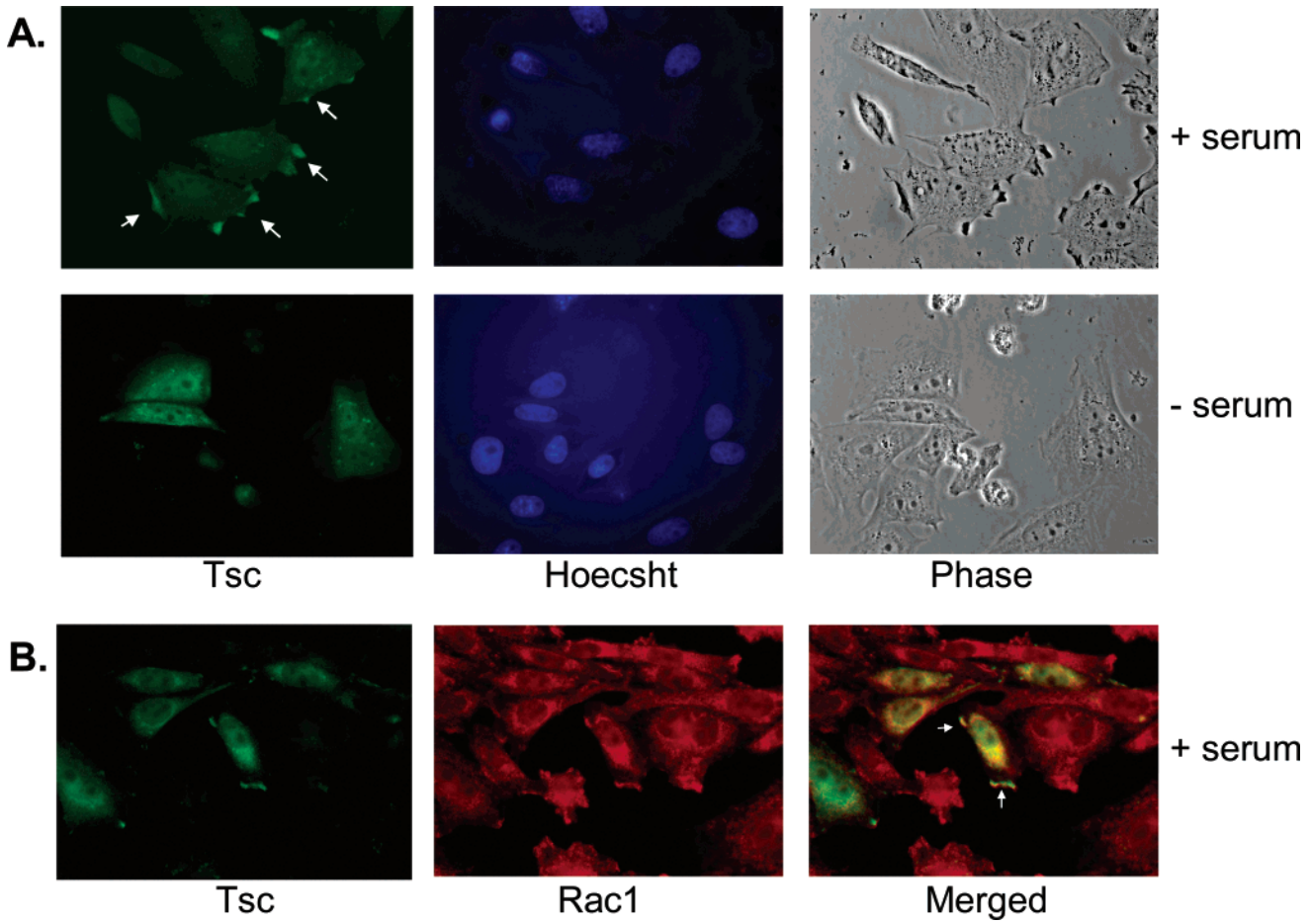

FIGURE 9: Tescalcin is localized to lamellipodia and membrane ruffles in CHO-K1 cells. (A) CHO-K1 cells were transfected with tescalcin cDNA (100 ng), and 24 h posttransfection, cells were incubated in the presence or absence of 10% fetal bovine serum for 18 h. Cells were subsequently immunostained for Tsc (green) or Hoechst (blue). Tescalcin localizes to membrane regions in the presence of serum. (B) Colocalization of tescalcin (green) and endogenous Rac-1 (red) to lamellipodia and membrane ruffles in the presence of serum. Images are representative of three independent experiments. Arrows denote location of lamellipodia/membrane ruffles.

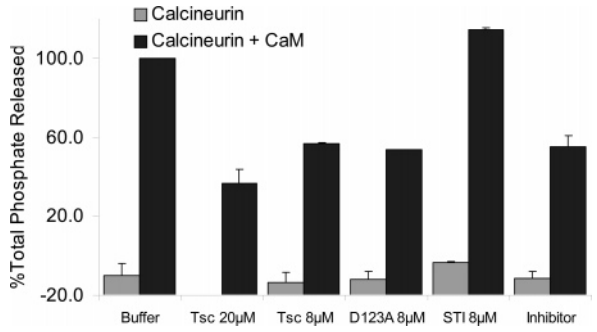

FIGURE 10: Inhibition of calcineurin phosphatase activity by tescalcin. Recombinant CnA/CnB heterodimer (±0.25 μM CaM) was incubated with control buffer (5 mM Tris and 50 mM NaCl); 8 or 20 μM tescalcin; 8 μM EF-hand D123A mutant; or 8 μM soybean trypsin inhibitor (STI). Soybean trypsin inhibitor acts as a negative control since this protein has a similar molecular weight and p*I* as tescalcin. As a positive control, a peptide inhibitor that resembles the autoinhibitory domain of CnA was used (40 μM). Studies for tescalcin were performed in quadruplicate, and for the inhibitors, in duplicate.

facilitates interaction with effectors or membrane compartments (*35*, *40*). Finally, we have shown that tescalcin is expressed in several cancer-derived cell lines, including HeLa, HL-60, and A549 (Figure 7A,C). Expression in these cancer cell lines may be significant since NHE-1, a putative binding partner of tescalcin, is associated with oncogenic transformation (*10*).

Subcellular fractionation of heart tissue and HeLa cells indicated that endogenous tescalcin was predominantly soluble and cytoplasmic (Figure 7E). Fluorescence microscopy confirmed these results, demonstrating that both endogenous and overexpressed tescalcin exist as cytosolic proteins (Figure 8). A common feature of Ca^{2+}-binding proteins is localization to the perinuclear region, which may represent a signaling microdomain since Ca^{2+} levels are especially high within this region (i.e., near the endoplasmic reticulum), where tescalcin is more likely to bind Ca^{2+} ions (*41*). We have also shown that mouse tescalcin localizes to lamellipodia and membrane ruffles (Figure 9), cellular compartments that are enriched with NHE, calcineurin A, and/or CHP1 (*15*, *37*, *42*). Localization of tescalcin to Rac-1-induced lamellipodia may result from its interaction with NHE. The role of NHE in lamellipodia may be to regulate cytoskeleton, cell adhesion, or motility (*37*), whereas CHP1 localization to the microtubule cytoskeleton may contribute to its role in vesicular trafficking (*8*, *14*).

Metal Ion Binding Properties of Tescalcin. Because about 30% of EF-hand domains fail to bind Ca^{2+}, it was not clear if tescalcin was capable of binding Ca^{2+} or other divalent cations (*30*). Mailander et al. (*19*) showed, by use of a $^{45}Ca^{2+}$ overlay, that human GST-tescalcin binds calcium . However, this method does not provide a measure of Ca^{2+} affinity and often has false positives with acidic proteins; tescalcin has

a predicted p*I* of 4.89. Using $^{45}Ca^{2+}$ equilibrium dialysis coupled with intrinsic tryptophan fluorescence, we reveal that tescalcin binds a single Ca^{2+} ion with submicromolar affinity (Figures 3 and 4). Further, we determine that the third EF-hand is responsible for Ca^{2+} coordination; this region has the strongest homology to the consensus EF-hand of the four total potential EF-hands in tescalcin (Figure 4A). Our study also reveals that, in a quiescent cell, tescalcin likely resides in an Mg^{2+}-bound form that may represent an "inactive" configuration. Upon cellular stimulation that increases intracellular Ca^{2+} to micromolar concentrations, Mg^{2+} might be replaced with Ca^{2+}, producing an "active" conformation. Tescalcin's conformational change is specific for Ca^{2+} and Mg^{2+}, since we demonstrated that the fluorescence does not change in the presence of Zn^{2+} ions. Although several Ca^{2+}-binding proteins including calmodulin undergo a large Ca^{2+}-mediated increase in α-helical content, tescalcin displayed very small alterations in secondary structure, which may result from binding only one Ca^{2+} ion (Figure 5). Myosin regulatory light chain, another protein with a single Ca^{2+}-binding site, also shows only a small increase in α-helical content (*32*). Though tescalcin binds only one Ca^{2+} ion at physiological concentrations, it likely bears three other helix−loop−helix regions that retain the EF-hand structure. As such, tescalcin may still bear intramolecular EF-hand pairing that stabilizes the EF-hand configuration and strengthens Ca^{2+} binding (*43*), as odd-numbered EF-hand proteins have weaker affinities (*44*).

The exact definition of an "EF-hand" is often ambiguous in the literature. If one defines an EF-hand by solely the existence of a helix−loop−helix, with acidic groups within the loop, then tescalcin has four EF-hands. However, if one considers an EF-hand not only by the amino acid sequence but also by its Ca^{2+} ion binding capacity, then tescalcin would have only a single EF-hand. We have chosen to define tescalcin as a protein that bears a single functional Ca^{2+} binding EF-hand, with three other "nonfunctional" ancestral EF-hands. Nevertheless, the tescalcin sequence is unique and represents one of only a handful of EF-hand-containing proteins binding a sole Ca^{2+} ion (*31*).

Potential Function of Tescalcin. Although this study did not determine the physiological function of tescalcin, we made the following advances toward this goal. First, we show that tescalcin binds calcium, and our Ca^{2+} affinity measurements exclude the possibility that tescalcin acts as a Ca^{2+} buffer (Figure 4C). Therefore, one model for tescalcin is a role as a calcium sensor that undergoes a Ca^{2+}-regulated conformational change that would allow Ca^{2+} to regulate protein−protein interactions, as occurs with calmodulin, recoverin, and many other EF-hand Ca^{2+}-binding proteins. At the same time, the small change in overall secondary structure in response to Ca^{2+} and lack of Ca^{2+} regulation on tescalcin's inhibition of calcineurin phosphatase activity or subcellular localization suggest that metal binding may instead impart stability, which may also explain the low levels of the EF-hand D123 mutant in mammalian cells when compared to wild-type tescalcin (Figure 6D). A structural rather than regulatory role for Ca^{2+} binding to tescalcin would not be surprising given its solitary EF-hand and the fact that EF-hand domains in CnB also play a structural role in stabilizing the catalytic subunit (*9*, *45*). Although the overall α-helical content undergoes very minor Ca^{2+}-induced changes, local changes in tertiary structure do occur, since Ca^{2+} binding to the EF-hand domain decreases the fluorescence of the tryptophan residue 49 amino acids away from the EF-hand domain.

The functional EF-hand of tescalcin is located in a similar region as the third EF-hand of calcineurin B (EF3). Interestingly, EF3 is a high-affinity Ca^{2+}-binding site that plays more of a structural rather than regulatory role (*45*); EF3 is located in the C-terminal region of CnB that forms contacts with CnA (*46*, *47*). The structural and functional characteristics of CnB's EF3 parallel our data regarding tescalcin's Ca^{2+}-binding EF-hand. In the absence of calmodulin, Ca^{2+} binding to CnB, including the EF3 region, only minimally stimulates the phosphatase activity of CnA (*45*, *47*, *48*). Binding of Ca^{2+} to EF3 also does not affect the ratio of recombinant CnA bound to CnB, and the presence of EGTA does not alter CnA−CnB binding (*45*, *48*); these observations correlate well with the inhibition of calcineurin by the D123A mutant (Figure 10). The homology of tescalcin's EF-hand with CnB's EF3 suggests that inhibition of calcineurin activity by tescalcin may be mediated by binding to CnA, thus utilizing a similar molecular mechanism of phosphatase inhibition as CHP1 (*13*).

As mentioned, tescalcin shares 35% identity with CHP-1, which may be significant as both proteins can inhibit CnA phosphatase activity and bind to the same effector, NHE1, in vitro (*13*, *16*, *19*). Further, tescalcin also displays similar subcellular compartmentalization in the perinuclear region and lamellipodia. However, in contrast to calcineurin B and CHP1, which are ubiquitous, tescalcin exhibits a restricted tissue expression pattern and binds only a single Ca^{2+} ion under physiological conditions. Although tescalcin was found to be overexpressed during gonadal development, this study illustrates that tescalcin can have a broader role in adult Ca^{2+} signaling and homeostasis in a variety of tissues and cell lines.

ACKNOWLEDGMENT

We extend our gratitude to Dr. James D. Potter (University of Miami) for the use of equipment and helpful discussions about the manuscript and to members of his laboratory, specifically Georgiana Guzman and David Dweck. In addition, we appreciate the laboratory assistance of Qiang Wang. We also thank Drs. Beatriz Fontoura, Saidas Nair, and Nagaraj Balasubramanian (University of Miami), and Dr. Diane Barber (UCSF) for valuable input and discussion.

REFERENCES

1. Perera, E. M., Martin, H., Seeherunvong, T., Kos, L., Hughes, I. A., Hawkins, J. R., and Berkovitz, G. D. (2001) *Endocrinology 142*, 455−63.
2. Roberts, L. M., Shen, J., and Ingraham, H. A. (1999) *Am. J. Hum. Genet. 65*, 933−42.
3. Melton, L. (2001) *Trends Endocrinol. Metab. 12*, 237−8.
4. Tilmann, C., and Capel, B. (2002) *Recent Prog. Horm. Res. 57*, 1−18.
5. Ikura, M. (1996) *Trends Biochem. Sci. 21*, 14−7.
6. Donato, R. (2001) *Int. J. Biochem. Cell Biol. 33*, 637−68.
7. Chin, D., and Means, A. R. (2000) *Trends Cell Biol. 10*, 322−8.
8. Barroso, M. R., Bernd, K. K., DeWitt, N. D., Chang, A., Mills, K., and Sztul, E. S. (1996) *J. Biol. Chem. 271*, 10183−7.
9. Rusnak, F., and Mertz, P. (2000) *Physiol. Rev. 80*, 1483−521.
10. Pang, T., Wakabayashi, S., and Shigekawa, M. (2002) *J. Biol. Chem. 10*, 10.

11. Ames, J. B., Hendricks, K. B., Strahl, T., Huttner, I. G., Hamasaki, N., and Thorner, J. (2000) *Biochemistry 39*, 12149−61.
12. Chen, C. K., Inglese, J., Lefkowitz, R. J., and Hurley, J. B. (1995) *J. Biol. Chem. 270*, 18060−6.
13. Lin, X., Sikkink, R. A., Rusnak, F., and Barber, D. L. (1999) *J. Biol. Chem. 274*, 36125−31.
14. Timm, S., Titus, B., Bernd, K., and Barroso, M. (1999) *Mol. Biol. Cell 10*, 3473−88.
15. Matsumoto, M., Miyake, Y., Nagita, M., Inoue, H., Shitakubo, D., Takemoto, K., Ohtsuka, C., Murakami, H., Nakamura, N., and Kanazawa, H. (2001) *J. Biochem. (Tokyo) 130*, 217−25.
16. Lin, X., and Barber, D. L. (1996) *Proc. Natl. Acad. Sci. U.S.A. 93*, 12631−6.
17. Pang, T., Su, X., Wakabayashi, S., and Shigekawa, M. (2001) *J. Biol. Chem. 276*, 17367−72.
18. Putney, L. K., Denker, S. P., and Barber, D. L. (2002) *Annu. Rev. Pharmacol. Toxicol. 42*, 527−52.
19. Mailander, J., Muller-Esterl, W., and Dedio, J. (2001) *FEBS Lett. 507*, 331−5.
20. Li, X., Liu, Y., Kay, C. M., Muller-Esterl, W., and Fliegel, L. (2003) *Biochemistry 42*, 7448−56.
21. Duronio, R. J., Jackson-Machelski, E., Heuckeroth, R. O., Olins, P. O., Devine, C. S., Yonemoto, W., Slice, L. W., Taylor, S. S., and Gordon, J. I. (1990) *Proc. Natl. Acad. Sci. U.S.A. 87*, 1506−10.
22. Potter, J. D., Strang-Brown, P., Walker, P. L., and Iida, S. (1983) *Methods Enzymol. 102*, 135−43.
23. Perrin, D. D., and Sayce, I. G. (1967) *Talanta 14*, 833−842.
24. Holroyde, M. J., Robertson, S. P., Johnson, J. D., Solaro, R. J., and Potter, J. D. (1980) *J. Biol. Chem. 255*, 11688−93.
25. Potter, J. D., and Gergely, J. (1975) *J. Biol. Chem. 250*, 4628−33.
26. Gill, S. C., and von Hippel, P. H. (1989) *Anal. Biochem. 182*, 319−326.
27. Chen, Y. H., and Yang, J. T. (1971) *Biochem. Biophys. Res. Commun. 44*, 1285−91.
28. Ramsby, M. L., and Makowski, G. S. (1999) *Methods Mol. Biol. 112*, 53−66.
29. Hashimoto, Y., Perrino, B. A., and Soderling, T. R. (1990) *J. Biol. Chem. 265*, 1924−7.
30. Kawasaki, H., and Kretsinger, R. H. (1994) *Calcium-binding proteins 1: EF-hands*, Academic Press, London.
31. Sugita, S., Ho, A., and Sudhof, T. C. (2002) *Neuroscience 112*, 51−63.
32. Szczesna, D., Guzman, G., Miller, T., Zhao, J., Farokhi, K., Ellemberger, H., and Potter, J. D. (1996) *J. Biol. Chem. 271*, 8381−6.
33. Lo, K. W., Zhang, Q., Li, M., and Zhang, M. (1999) *Biochemistry 38*, 7498−508.
34. Carrion, A. M., Link, W. A., Ledo, F., Mellstrom, B., and Naranjo, J. R. (1999) *Nature 398*, 80−4.
35. Faurobert, E., Chen, C. K., Hurley, J. B., and Teng, D. H. (1996) *J. Biol. Chem. 271*, 10256−62.
36. Ascoli, G. A., Luu, K. X., Olds, J. L., Nelson, T. J., Gusev, P. A., Bertucci, C., Bramanti, E., Raffaelli, A., Salvadori, P., and Alkon, D. L. (1997) *J. Biol. Chem. 272*, 24771−9.
37. Denker, S. P., Huang, D. C., Orlowski, J., Furthmayr, H., and Barber, D. L. (2000) *Mol. Cell. 6*, 1425−36.
38. Su, Q., Zhao, M., Weber, E., Eugster, H. P., and Ryffel, B. (1995) *Eur. J. Biochem. 230*, 469−74.
39. Lai, M. M., Burnett, P. E., Wolosker, H., Blackshaw, S., and Snyder, S. H. (1998) *J. Biol. Chem. 273*, 18325−31.
40. Burgoyne, R. D., and Weiss, J. L. (2001) *Biochem. J. 353*, 1−12.
41. Lollike, K., Johnsen, A. H., Durussel, I., Borregaard, N., and Cox, J. A. (2001) *J. Biol. Chem. 276*, 17762−9.
42. Oliveria, S. F., Gomez, L. L., and Dell'Acqua, M. L. (2003) *J. Cell. Biol. 160*, 101−12.
43. Niki, I., Yokokura, H., Sudo, T., Kato, M., and Hidaka, H. (1996) *J. Biochem. (Tokyo) 120*, 685−98.
44. Day, I. S., Reddy, V. S., Shad Ali, G., and Reddy, A. S. (2002) *Genome Biol. 3*, 0056.1−0056.24.
45. Feng, B., and Stemmer, P. M. (1999) *Biochemistry 38*, 12481−9.
46. Griffith, J. P., Kim, J. L., Kim, E. E., Sintchak, M. D., Thomson, J. A., Fitzgibbon, M. J., Fleming, M. A., Caron, P. R., Hsiao, K., and Navia, M. A. (1995) *Cell 82*, 507−22.
47. Feng, B., and Stemmer, P. M. (2001) *Biochemistry 40*, 8808−14.
48. Stemmer, P. M., and Klee, C. B. (1994) *Biochemistry 33*, 6859−66.
49. Corpet, F. (1988) *Nucleic Acids Res. 16*, 10881−90.

BI034870F